Journal of Catalysis 268 (2009) 165–174

Contents lists available at ScienceDirect

Journal of Catalysis

journal homepage: www.elsevier.com/locate/jcat

A molecular insight into propylene epoxidation on Cu/SiO_2 catalysts using O_2 as oxidant

Weiguang Su, Shouguo Wang, Pinliang Ying, Zhaochi Feng, Can Li *

State Key Laboratory of Catalysis, Dalian Institute of Chemical Physics, Chinese Academy of Sciences, P.O. Box 110, Dalian 116023, China

ARTICLE INFO

Article history:
Received 16 June 2009
Revised 20 September 2009
Accepted 21 September 2009
Available online 21 October 2009

Keywords:
C_3H_6 epoxidation
Cu/SiO_2
Propylene oxide
IR spectroscopy
Cu^0 or Cu^+ species
Potassium acetate (KAc) modification

ABSTRACT

We investigated the catalytic performances of Cu/SiO_2 with various promoters on the epoxidation of C_3H_6 by O_2. Propylene oxide (PO) is the only product at reaction temperatures below 500 K and the rate of PO formation can reach 2.5 mmol g^{-1} h^{-1} over the potassium acetate (KAc)-Cu/SiO_2 catalyst. IR studies show that both Cu^0 and Cu^+ in Cu/SiO_2 can activate the C=C bond of C_3H_6, and π donation of C_3H_6 to Cu^0 or Cu^+ also results in a red shift of ν_{CO} with respect to CO adsorbed on Cu^0 or Cu^+ "solo". However, C_3H_6 is only weakly adsorbed on Cu^{2+}. Both Cu^0 and Cu^+ species show C_3H_6 epoxidation activity. It is proposed that the isolated Cu species and small CuO_x clusters with low valence state (Cu^0 or Cu^+) modified by KAc are the main active sites for C_3H_6 epoxidation on Cu/SiO_2 catalyst with O_2 as the oxidant.

1. Introduction

Propylene oxide (PO) is one of the important building blocks in chemical industry. Until now, the major conventional manufacturing methods of PO are the chlorohydrin process and the Halcon process. The chlorohydrin process is being phased out because of environmental pollution, while the latter has the byproduct limitation [1]. Therefore, it becomes urgent to establish a direct and green epoxidation route for PO production. Many studies focused on producing PO with novel methods, for example, the TS-1/H_2O_2 system [2,3] and *in situ*-generated hydrogen peroxide systems such as gold supported on titania [4,5], as well as using N_2O [6–8] as the oxidant. However, the high cost of these oxidants or the low efficiency of H_2 utilization [5] limits the commercialization of these processes. The most ideal process is the epoxidation of propylene with molecular oxygen as the oxidant. The epoxidation of ethylene by O_2 has been commercialized for several decades using Ag-based catalysts, but the epoxidation of propylene by O_2 is not successful [9]. Many research efforts have also been paid to Ag-based and Cu-based catalysts in propylene epoxidation by O_2, but PO selectivity can hardly exceed 50% even at very low propylene conversion [10–18]. The main reason for the low PO selectivity is that the allylic hydrogen atoms react more easily with the nucleophilic oxygen species resulting in the byproducts and final production of CO_x [19]. Thus, the epoxidation of C_3H_6 using O_2 remains one of the most challenging goals in catalysis field.

Through a series of surface chemistry studies on Ag and Cu single-crystal surfaces under ultrahigh vacuum conditions, Cropley et al. [20,21] and Lambert et al. [22] have suggested that Cu is more selective than Ag for the epoxidation of higher alkenes with allylic C–H bonds by preadsorbed oxygen atoms. The lower basicity of the oxygen atoms on metallic Cu may favor its epoxidation selectivity [23]. On the other hand, Monnier and Hartley [24] have pointed out that metallic Cu (Cu^0) is difficult to function as a true epoxidation catalyst because it may be readily oxidized under reaction conditions into Cu_2O or CuO, which is believed to be nonselective. In fact, only very few studies to date have reported the epoxidation of C_3H_6 by O_2 with Cu-based samples as true catalysts [17,18,25–28]. In our previous work, Lu et al. [17] reported a PO selectivity of 43% at 0.19% C_3H_6 conversion over a NaCl-modified $VCe_{1-x}Cu_x$ oxide catalyst, with a maximum PO formation rate of 0.17 mmol g^{-1} h^{-1}. NaCl-modified Cu/SiO_2 showed a PO selectivity of 44% at 0.16% C_3H_6 conversion and a maximum PO formation rate of 0.19 mmol g^{-1} h^{-1} [18]. Vaughan et al. [25] showed that Cu/SiO_2 prepared by a microemulsion technique without NaCl additive could obtain 53% PO selectivity at 0.25% C_3H_6 conversion and a PO formation rate of 0.014 mmol g^{-1} h^{-1} under their reaction conditions. Recently, Chu et al. [26] have reported a halogen-free K^+-modified CuO_x/SBA-15 prepared by an impregnation method and Zhu et al. [27] have reported a K^+-modified CuO_x/SiO_2 prepared by a sol–gel method, both of them could catalyze C_3H_6 epoxidation efficiently especially under O_2-rich conditions (PO_2/PC_3H_6 = 98.8/2.5).

---

* Corresponding author. Fax: +86 411 84694447.
E-mail address: canli@dicp.ac.cn (C. Li).
URL: http://www.canli.dicp.ac.cn (C. Li).

0021-9517/$ - see front matter © 2009 Elsevier Inc. All rights reserved.
doi:10.1016/j.jcat.2009.09.017

The decline of PO selectivity with increasing C_3H_6 conversion was much slow compared with other reported Cu-based catalysts. They obtained a PO selectivity of 55% at 1.4% C_3H_6 conversion and a PO formation rate of 2.2 mmol g^{-1} h^{-1} (TOF, ca. 18 h^{-1}). In addition, they proposed that Cu^+ could function as the active site for the epoxidation of C_3H_6 by O_2 [27].

Until now, although much effort has been made in the C_3H_6 epoxidation by O_2 over Cu-based catalysts, there are many discrepancies on the active sites for C_3H_6 epoxidation, and the effect of the valence state and the size of Cu species on the catalytic performances are not clear. In the present work, the catalytic performances of Cu/SiO_2 with different promoters for C_3H_6 epoxidation by O_2 were studied using the fixed bed catalytic reactor. The adsorption and activation of C_3H_6 on Cu/SiO_2 were examined by IR spectroscopy using CO and NO as molecular probes. To the best of our knowledge, this is the first time to correlate the results of C_3H_6 epoxidation reaction with those of IR spectra of adsorbed C_3H_6 on Cu/SiO_2 catalysts. We found that C_3H_6 is strongly adsorbed on Cu^0 and Cu^+ via its C=C double bond, and both Cu^0 and Cu^+ can catalyze the epoxidation of C_3H_6 to form PO. Promoters especially KAc can largely enhance PO selectivity and yield, while the adsorption of C_3H_6 on Cu species is nearly independent of the promoters investigated in this work. Finally, the size effect of CuO nanoparticles on the catalytic performances of C_3H_6 epoxidation was also studied, and the catalyst with small CuO nanoparticles (≈2.9 nm) is found to be most beneficial to PO formation.

2. Experimental

2.1. Catalyst preparation

Cu/SiO_2 catalyst (~9 wt%) was prepared by homogeneous deposition-precipitation method [29,30]. The Cu/SiO_2 catalyst was prepared by a suspension of silica in water containing the appropriate amounts of aqueous $Cu(NO_3)_2$ and urea, the molar ratio of $Cu(NO_3)_2$/urea is 1/10. The initial pH of the well-stirred suspension was adjusted to 2 by addition of nitric acid. The suspension was subsequently heated to 363 K and kept at this temperature for 40 h. At 363 K the hydrolysis of urea results in a homogeneous pH-rise causing precipitation of the copper ions. After completion of the precipitation at a pH of about 7, the precursor was obtained by filtration, and washed with distilled water. After drying for 60 h at 393 K, the powdery sample was calcined at 723 K in air for 10 h to obtain the Cu/SiO_2. The promoter-modified Cu/SiO_2 samples were prepared by impregnation of the calcined Cu/SiO_2 with an aqueous solution of promoter followed by drying and calcination at 723 K for 4 h. These samples are named as (promoter)-Cu/SiO_2 (the molar ratio of promoter to Cu is about 0.4).

For comparison, a Cu/SiO_2 sample with the same loading of Cu was prepared by incipient wetness impregnation of the silica support with aqueous $Cu(NO_3)_2$ followed by drying in air (12 h, 393 K) and air calcination (5 h, 573 K), this sample is identified as Cu/SiO_2 (IMP573).

2.2. Catalyst characterization

Powder X-ray diffraction patterns were obtained on a Rigaku MiniFlex diffractometer with a Cu Kα radiation source. Diffraction patterns were collected from 5° to 90° at a speed of 5°/min. TEM was taken on a JEM-2011 TEM for estimating the particle size and morphology. UV–Vis diffuse reflectance spectra were recorded on a JASCO V-550 UV–Vis spectrophotometer.

XPS spectra were obtained in a VG ESCALAB MK2 spectrometer, and base pressure is 2×10^{-8} Pa. Al Kα radiation was used as excitation source and spectra were energy calibrated by taking Si2p peak at 103.4 eV (BE).

The Cu/SiO_2 samples were pressed into self-supporting wafers (ca. 10 mg/cm^2) and mounted inside an IR cell with two CaF_2 windows for FT-IR spectroscopy. IR experiments were then performed as follows:

(1) CO and C_3H_6 coadsorption on Cu^+. Prior to the adsorption measurements, the Cu/SiO_2 samples were activated by evacuation at 673 K for 180 min, subsequently cooled to the desired temperature. Previous literature results show that evacuation at high temperature for Cu-containing samples can result in the autoreduction of most Cu^{2+} to Cu^+ [31].
(2) CO and C_3H_6 coadsorption on Cu^0. The Cu/SiO_2 samples in the IR cell were reduced by H_2 at 673 K for 120 min, and evacuated at the same temperature for 90 min. After heating, the sample was cooled to room temperature (ca. 300 K), and the gas dosing experiments were carried out.
(3) NO and C_3H_6 coadsorption on Cu^{2+}. The Cu/SiO_2 samples were heated to 673 K in O_2 for 180 min, subsequently cooled to room temperature (ca. 300 K) in O_2. The O_2 was evacuated at room temperature for several minutes, and the adsorption measurements were done.

All infrared spectra were collected with a resolution of 4 cm^{-1} and 64 scans by a Fourier transform infrared spectrometer (Nicolet NEXUS 470) with an MCT detector. All the spectra shown here were in the absorbance mode, and their backgrounds were recorded before admitting the adsorbed gas under corresponding experimental conditions of the spectra.

2.3. Catalyst testing

The catalytic epoxidation of propylene was carried out in a microreactor system under atmospheric pressure. Oxygen was used as oxidant. Before the reaction, the catalyst was pretreated with different gas (N_2, H_2, or O_2) for 60 min at 673 K. Reaction products were analyzed with online GC analysis. Two GCs were used: a GC920 with an FID detector and AT-WAX capillary column (50 m × 0.32 mm i.d. × 0.30 μm) and a GC7890II with a TCD detector and Porapak Q-packed column, both the AT-WAX and the Porapak Q with 333 K as initiate temperature. The method of carbon balance was used.

3. Results and discussion

3.1. UV–Vis, XRD, and TEM characterization of Cu/SiO_2 catalysts

Fig. 1 shows the UV–Vis diffuse reflectance spectra of the Cu/SiO_2 samples. The SiO_2 support shows a strong absorption band at 230 nm, this band may be due to the charge transfer of ligand to minim impurity, such as Fe^{3+} in SiO_2 [32]. For Cu/SiO_2 catalyst, several new bands appeared at 254, 302, and 760 nm are assigned to the charge-transfer transitions of the ligand O^{2-} to isolated metal center Cu^{2+}, and small CuO clusters, and the d–d transition of CuO particles, respectively [33–35]. When the Cu/SiO_2 sample was modified with potassium acetate (KAc) or sodium acetate (NaAc), the feature of the UV–Vis spectra is almost the same, suggesting that the electronic absorption properties of Cu species is hardly changed after the modification with K^+ or Na^+. However, when the Cu/SiO_2 sample was modified with KCl or NaCl, the intensity of the band at 760 nm is greatly enhanced. The UV–Vis spectra are very similar to those of the Cu/SiO_2 (IMP573) sample which is expected to have large CuO particles. These results suggest that the Cu species is agglomerated to form massive CuO particles after Cu/SiO_2 was modified with KCl or NaCl. Previous literature [36] showed that Cl^- could result in the agglomeration of the Au species during the calcination process, so the

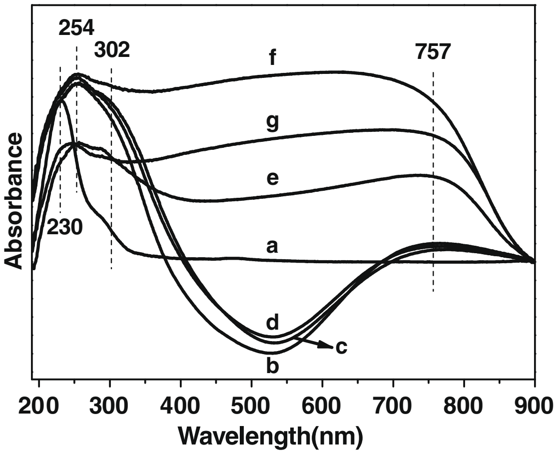

Fig. 1. UV–Vis diffuse reflectance spectra of the Cu/SiO_2 samples. (a) SiO_2, (b) Cu/SiO_2, (c) (KAc)–Cu/SiO_2, (d) (NaAc)–Cu/SiO_2, (e) (KCl)–Cu/SiO_2, (f) (NaCl)–Cu/SiO_2, (g) Cu/SiO_2 (IMP573).

agglomeration of CuO particles may be induced by the presence of Cl^- ions.

The XRD patterns of Cu/SiO_2 samples are displayed in Fig. 2. The XRD pattern of Cu/SiO_2 only shows a broad and weak peak centered at 22.5°, which is due to the diffraction of amorphous SiO_2 powder. This indicates that CuO species is highly dispersed on SiO_2 support (the color of Cu/SiO_2 is green). After a modification of Cu/SiO_2 with KAc or NaAc, the XRD patterns are still unaltered. However, when Cu/SiO_2 was modified with KCl or NaCl, except for crystalline KCl ($2\theta = 28.3°$ and 40.5°, JCPDS Number 75-0296) or NaCl (31.7° and 45.4°, JCPDS Number 78-0751), sharp peaks at $2\theta = 35.3°$, 38.4°, and 48.6° are observed. All these peaks are attributed to crystalline CuO (JCPDS Number 80-1917). The XRD pattern of Cu/SiO_2 (IMP573) also shows evident diffraction peaks of crystalline CuO. The results of UV–Vis spectra and XRD patterns of Cu/SiO_2 samples are in good agreement with each other. Both K^+ and Na^+ ions have little effect on the crystalline size of CuO, while Cl^- ions can result in the agglomeration of the Cu species, forming bulk CuO.

Fig. 3 shows the TEM images of Cu/SiO_2 samples. For Cu/SiO_2 sample, the mean size of CuO nanoparticles is about 2.9 nm, which is much smaller than that of 5 wt% CuO_x–SiO_2 (17 nm) prepared by the sol–gel method reported by Zhu et al. [27]. After a modification with K^+ or Na^+ ions, the TEM images reveal that the mean size of CuO is still about 3 nm. TEM observations show that the CuO species is agglomerated from ~3 to ~15 nm after the modification by KCl or NaCl (Fig. 3d and e). Accordingly, the results of UV–Vis spectra, XRD patterns, and TEM images are well consistent with each other.

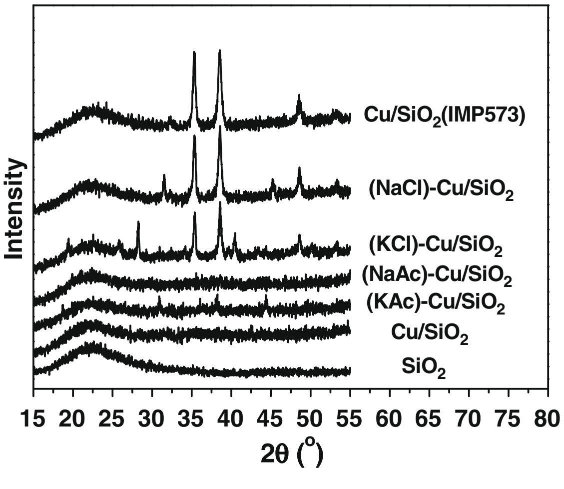

Fig. 2. XRD patterns of Cu/SiO_2 samples with and without promoter modification.

3.2. Catalytic performances of Cu/SiO_2 catalysts for C_3H_6 epoxidation reaction

Fig. 4 displays the catalytic performances of C_3H_6 epoxidation by O_2 over the Cu/SiO_2 catalysts. Before the reaction, the Cu/SiO_2 catalysts were pretreated in N_2 at 673 K. The results of XPS spectra show that surface Cu^+ species is nearly 90% for each catalyst under this pretreatment (Supplementary material, Table S1 and Fig. S1). Compared with Cu/SiO_2, (KAc)–Cu/SiO_2 and (NaAc)–Cu/SiO_2 catalysts show much higher PO selectivity. Among all promoters used in the catalysts, the catalysts modified with KAc and NaAc show the highest PO selectivity (100%) at the initial stage of C_3H_6 selective oxidation reaction. For the Cu/SiO_2 catalyst, PO selectivity of 22% can be obtained only at C_3H_6 conversion of 0.64%. With the increase of C_3H_6 conversion to >1% by raising the reaction temperatures, the PO selectivity is dramatically decreased to <5%. When NaCl was used as a promoter, PO selectivity can be elevated to 62% despite the lower C_3H_6 conversion. From the above results, Cl^- ions can cause the agglomeration of the Cu species, and the decrease of the concentration of Cu^+ may result in the lower C_3H_6 conversion. The reason for that the PO selectivity is decreased after the modification by KCl compared with Cu/SiO_2 catalyst is not clear at the moment. When the Cu/SiO_2 sample was modified by KAc or NaAc, an interesting phenomenon is observed. PO is the only product at lower C_3H_6 conversion. Thus, KAc or NaAc modification switches the formation of acrolein to that of PO. With increasing C_3H_6 conversion by elevating reaction temperatures, the PO selectivity decreases monotonously. However, 40% PO selectivity can still be sustained with C_3H_6 conversion of 1% on (KAc)–Cu/SiO_2. This result is comparable to the best results reported on Cu-based catalysts for C_3H_6 epoxidation by O_2. Furthermore, the decrease of PO selectivity for (KAc)–Cu/SiO_2 is obviously slower than that for (NaAc)–Cu/SiO_2. From Fig. 4, the effect of the promoters on both PO selectivity and C_3H_6 conversion increases in the order: KCl < NaCl < NaAc < KAc.

Fig. 5 summarizes C_3H_6 conversion and PO selectivity as a function of reaction temperature over the Cu/SiO_2 catalysts which were reduced by H_2 at 673 K before reaction. Only Cu^0 species is present on catalyst surfaces according to the results of XPS spectra (Supplementary material, Table S2 and Fig. S2). For Cu/SiO_2, (KCl)–Cu/SiO_2, and (NaCl)–Cu/SiO_2 catalysts, the highest PO selectivity hardly exceeds 50%, and more than 30% PO selectivity can be obtained at C_3H_6 conversion <1%. The increase of C_3H_6 conversion to >1% remarkably decreases PO selectivity to <10%. In the cases of (KAc)–Cu/SiO_2 and (NaAc)–Cu/SiO_2 catalysts, PO selectivity is significantly improved, and 100% PO selectivity is obtained at ~0.2% C_3H_6 conversion. These results are much better than those on Cu-based catalysts reported previously [17,18,25,26]. The promoters such as KAc and NaAc can greatly enhance the selectivity to PO. For (KAc)–Cu/SiO_2 and (NaAc)–Cu/SiO_2 catalysts, PO selectivity also decreases gradually with the increase of C_3H_6 conversion by raising the reaction temperatures. Acrolein and CO_x are the main oxidation products at higher reaction temperatures. It is worthy to mention that 61.1% PO selectivity can still be sustained at 1.35% C_3H_6 conversion over (KAc)–Cu/SiO_2 catalyst. It is clear that (KAc)–Cu/SiO_2 catalyst exhibits the highest PO selectivity at the same level of C_3H_6 conversion among all the catalysts tested.

The above results show that irrespective of the pretreatment atmosphere (in N_2 or H_2), KAc is the best modifier for PO formation among all the modifiers investigated in this work. Comparing the

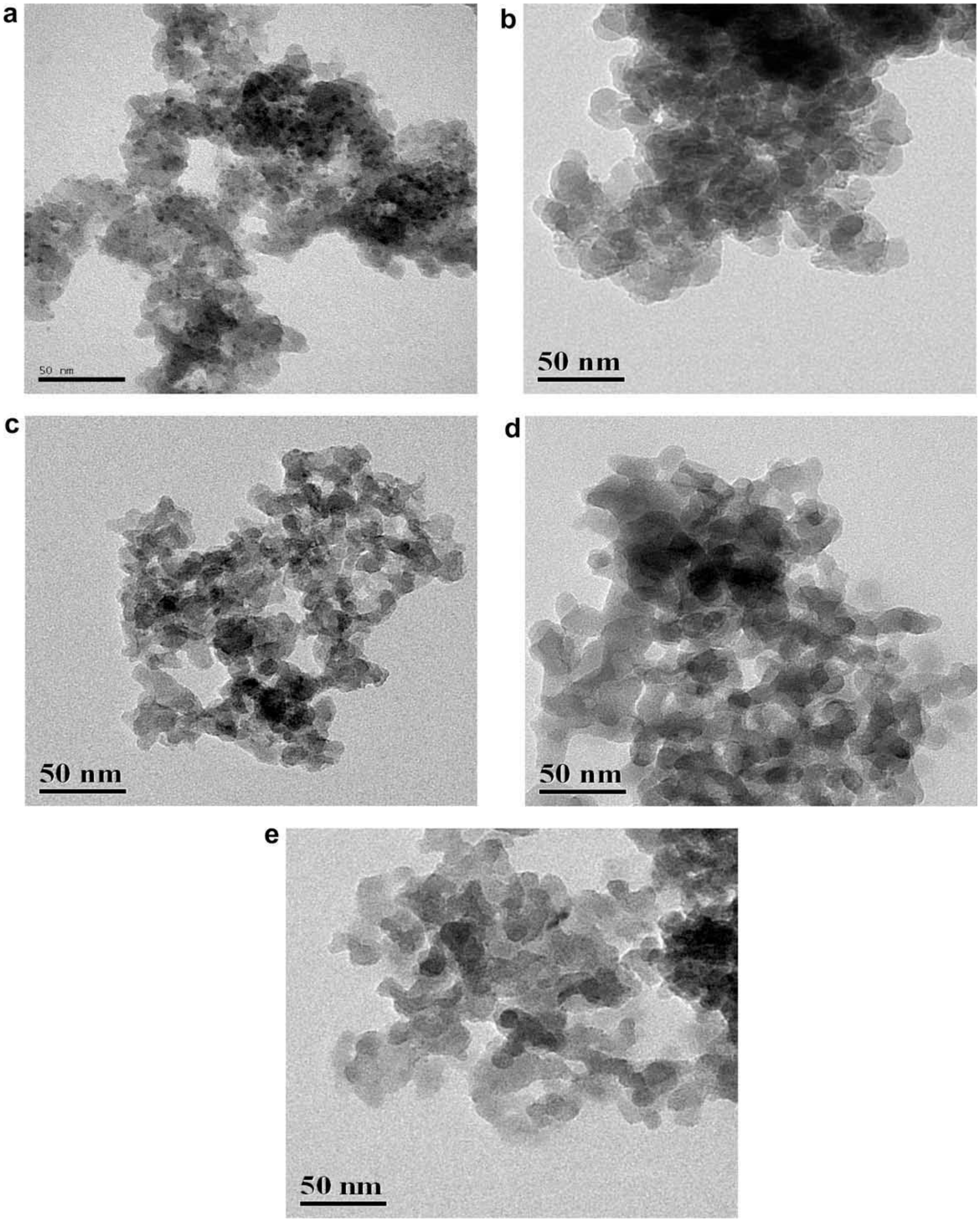

Fig. 3. TEM images of the Cu/SiO_2 samples. (a) Cu/SiO_2, (b) (KAc)–Cu/SiO_2, (c) (NaAc)–Cu/SiO_2, (d) (KCl)–Cu/SiO_2, and (e) (NaCl)–Cu/SiO_2.

catalytic performances for C_3H_6 epoxidation over (KAc)–Cu/SiO_2 catalyst treated in N_2 and (KAc)–Cu/SiO_2 reduced in H_2, PO selectivity for both catalysts is higher at lower C_3H_6 conversion. However, with the increase of C_3H_6 conversion, the decrease of PO selectivity for the catalyst with H_2 reduction is much slower than that for that with N_2 pretreatment. It seems that Cu^0 species is more favorable for PO formation than Cu^+. Namely, the reduced Cu species is more active for the epoxidation of C_3H_6 by O_2 although the Cu species may be oxidized under reaction conditions.

Table 1 shows the catalytic performances of the Cu/SiO_2 catalysts which were oxidized by O_2 at 673 K before reaction. Cu^{2+} species is predominant in Cu/SiO_2 catalysts in this instance (Supplementary material, Table S3 and Fig. S3). All the Cu/SiO_2 catalysts have much low epoxidation activity except for (KAc)–Cu/SiO_2 catalyst. 19.1% PO selectivity is obtained only at 0.27% C_3H_6 conversion for (KAc)–Cu/SiO_2 catalyst. Over all the Cu/SiO_2 catalysts, acrolein is the main partial oxidation product as well as a portion of combustion product of CO_x. These results are quite different from those of Cu/SiO_2 catalysts pretreated in N_2 or H_2. It seems that the pretreatment of Cu/SiO_2 catalysts by O_2 is very unfavorable for PO formation. The oxidized Cu species with high valence state (Cu^{2+}) always produce acrolein and CO_x.

To gain further insight into the role of KAc, we compared the catalytic performances of the Cu/SiO_2 and (KAc)–Cu/SiO_2 catalysts at different reaction temperatures. Figs. 6 and 7 show the reaction

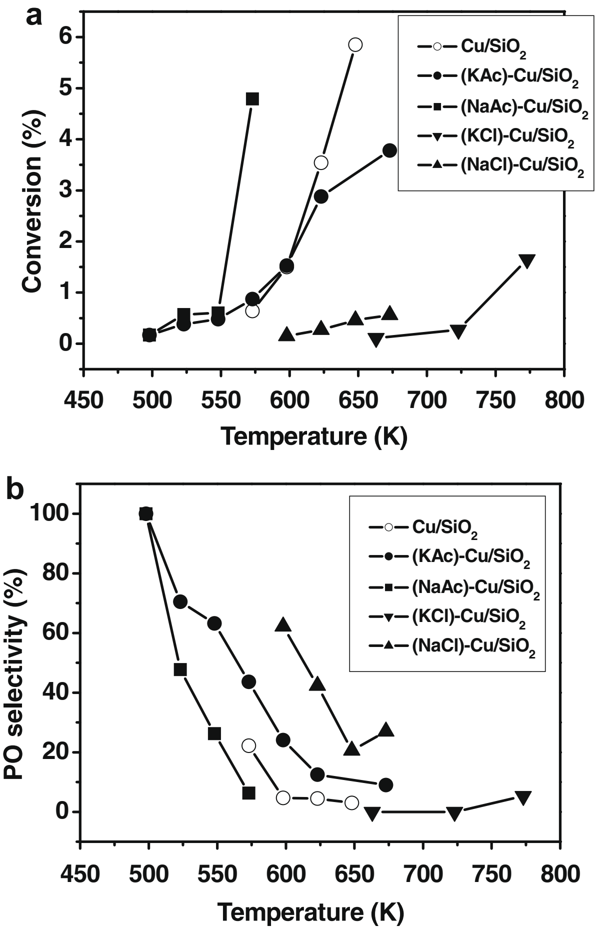

Fig. 4. C_3H_6 conversion (a) and PO selectivity (b) as a function of reaction temperature over the Cu/SiO_2 catalysts pretreated by N_2 at 673 K. Reaction conditions: catalyst volume, 0.2 ml; $C_3H_6:O_2:N_2 = 1:1:15$; Space velocity = 30,000 h^{-1}.

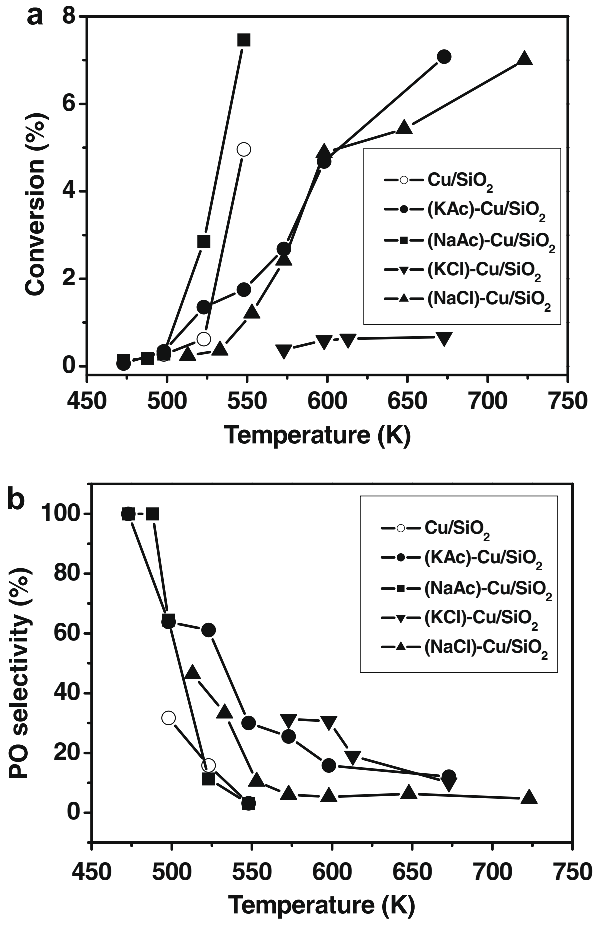

Fig. 5. C_3H_6 conversion (a) and PO selectivity (b) as a function of reaction temperature over the Cu/SiO_2 catalysts pretreated by H_2 at 673 K. Reaction conditions: catalyst volume, 0.2 ml; $C_3H_6:O_2:N_2 = 1:1:15$; Space velocity = 30,000 h^{-1}.

results of the two catalysts pretreated in N_2 and H_2, respectively. In both cases over Cu/SiO_2, acrolein is the main partial oxidation product even at very low C_3H_6 conversion. CO_x is the main product (60–80%) at higher reaction temperatures. However, after KAc modification, although C_3H_6 conversion is decreased, the selectivity to PO is increased significantly to 30–100% at lower reaction temperatures and the selectivity to acrolein is in the ranges of 20–40%. At higher reaction temperatures, the selectivity to CO_x exceeds 50%, this may be due to the oxidation of the Cu species by O_2 during the reaction process (Supplementary material, Fig. S5). Even at the same reaction temperature, the selectivity to CO_x is decreased by about 25% compared with Cu/SiO_2. Thus, KAc modification switches the formation of a part of acrolein to that of PO at lower reaction temperatures and suppresses the formation of CO_x at higher reaction temperatures. According to the previous literature [27], we consider that KAc modification neutralizes the Lewis acidity on Cu/SiO_2 catalyst surface, which should contribute to the inhibition of the isomerization of PO because it is known that epoxides would easily undergo isomerization over an acidic catalyst surface [37].

3.3. IR spectra of adsorbed C_3H_6 on Cu/SiO_2 with different valence states of Cu species

In order to figure out the role of different pretreatment methods in the catalytic performances of C_3H_6 epoxidation, we also performed IR studies of the adsorption and activation of C_3H_6 on Cu/SiO_2 catalyst with different valence states of Cu species. CO and NO may be used as molecular probes to follow the electron-donating abilities of the adsorption sites [38–40]. The IR experimental details were described in experimental section. Fig. 8 displays the IR spectra of CO and C_3H_6 coadsorbed on Cu^0 and Cu^+ as well as NO and C_3H_6 coadsorbed on Cu^{2+} in Cu/SiO_2 catalyst. It is well known that CO and NO are the most useful molecular probes for monitoring the oxidation state of small Cu nanoparticles. CO is adsorbed strongly on Cu^+ or Cu^0 sites, but it is hardly adsorbed on Cu^{2+} sites at room temperature [41]. On the other hand, NO is preferentially adsorbed on Cu^{2+} sites [42]. Thus, we are able to study the adsorption and activation of C_3H_6 on different valence states of Cu species with the two molecular probes by IR spectroscopy. When CO is adsorbed on Cu^0/SiO_2 (H_2 reduction), a broad and strong band at 2103 cm^{-1} is observed, which is due to the C–O stretching vibration of Cu^0CO species [41]. After introducing C_3H_6 gas, the IR band is red shifted from 2103 to 2084 cm^{-1} ($\Delta\nu = 19$ cm^{-1}) and the intensity of the IR band greatly decreases. This result indicates that C_3H_6 donates its π electrons to Cu^0, which results in a stronger π-back donation of d electrons of Cu^0 to anti-bonding π^* orbitals of CO [43]. The decrease in intensity implies that most CO molecules in Cu^0CO forms are replaced by C_3H_6. A weak band at 2126 cm^{-1} is also detected, which may be due to adsorbed CO on Cu^+ [41]. In the case of Cu^+ (evacuation at 673 K, this pretreatment can produce mostly Cu^+ according to the literature [31]), similar experimental results are obtained. Adsorbed CO

Table 1
Catalytic performances of C_3H_6 epoxidation over different Cu/SiO_2 catalysts pretreated by O_2 at 673 K.

Catalyst	T (K)	C_3H_6 conv. (%)	Selectivity (%)			
			PO	Acetaldehyde	Acrolein	CO_x
Blank	673	None	0	0	0	0
SiO_2	673	0.10	0	0	100	0
Cu/SiO_2	573	0.54	0	0	72.2	27.8
	598	2.58	0	5.3	41.9	52.8
	623	8.17	0	3.6	30.2	66.2
(KAc)–Cu/SiO_2	598	0.27	19.1	0	80.9	0
	623	0.82	8.2	0	74.6	17.2
	648	1.61	5.2	0	56.6	38.2
(NaAc)–Cu/SiO_2	598	0.37	0	0	100	0
	623	1.04	0	0	78.2	21.8
	648	2.25	5.0	3.1	53.3	38.6
(KCl)–Cu/SiO_2	723	0.17	0	0	100	0
	773	1.02	0	0	62.4	37.6
(NaCl)–Cu/SiO_2	673	0.21	0	0	100	0
	723	0.56	0	0	81.3	18.7
	773	0.87	0	0	75.4	24.6

Reaction conditions: catalyst volume, 0.2 ml; $C_3H_6:O_2:N_2 = 1:1:15$; Space velocity = 30,000 h^{-1}.

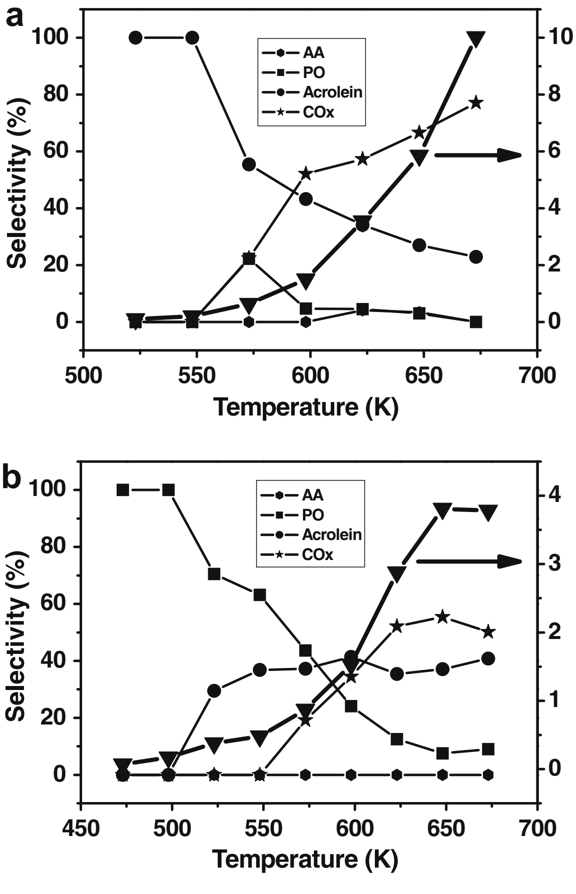

Fig. 6. Temperature dependences on catalytic performances of (a) Cu/SiO_2 and (b) (KAc)–Cu/SiO_2 with N_2 pretreatment for the oxidation of C_3H_6 by O_2. Reaction conditions: catalyst volume, 0.2 ml; $C_3H_6:O_2:N_2 = 1:1:15$; Space velocity = 30,000 h^{-1}.

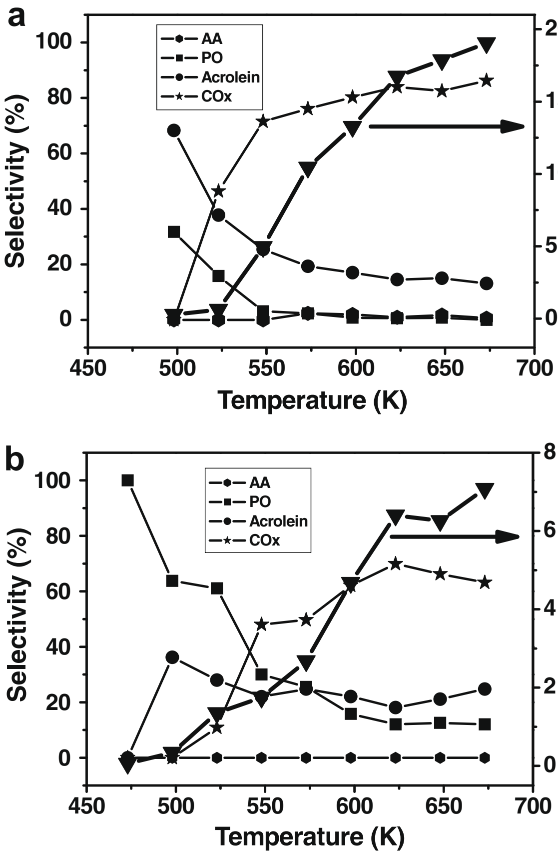

Fig. 7. Temperature dependences on catalytic performances of (a) Cu/SiO_2 and (b) (KAc)–Cu/SiO_2 with H_2 pretreatment for the oxidation of C_3H_6 by O_2. Reaction conditions: catalyst volume, 0.2 ml; $C_3H_6:O_2:N_2 = 1:1:15$; Space velocity = 30,000 h^{-1}.

produces a sharp and strong peak at 2136 cm^{-1} which is assigned to CO adsorbed on Cu^+ [41]. The coadsorption of C_3H_6 results in a sharp decrease in intensity of the band at 2136 cm^{-1}, and a red shift of C–O band from 2136 to 2126 cm^{-1} ($\Delta v = 10\ cm^{-1}$). The reason is the same as that for Cu^0. When NO is adsorbed on Cu^{2+}, a relatively weak band at 1890 cm^{-1} appears [42]. Unlike Cu^0 and Cu^+, the band at 1890 cm^{-1} remains almost the same after introducing C_3H_6, which shows that C_3H_6 is weakly adsorbed on Cu^{2+}.

Fig. 9 shows the IR spectra of C_3H_6 adsorbed on Cu^+, Cu^{2+}, and Cu^0 in Cu/SiO_2, respectively. For comparison, the IR spectra of gas phase C_3H_6 and C_3H_6 physically adsorbed on SiO_2 are also presented (the pressure of C_3H_6 is about 270 Pa). The IR spectra of adsorbed C_3H_6 on Cu^0 and Cu^{2+} are almost the same as those on SiO_2 and gas phase C_3H_6. However, in the case of Cu^+, two new bands at 1541 and 1456 cm^{-1} are observed. The band at 1541 cm^{-1} is a characteristic feature due to C=C of C_3H_6 interaction with Cu^+

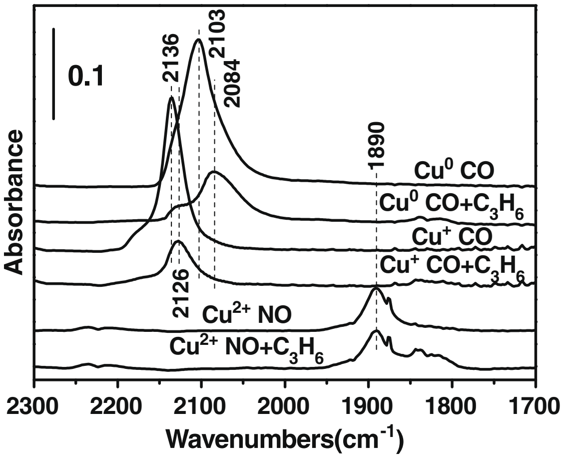

Fig. 8. IR spectra of CO and C_3H_6 coadsorbed on Cu^0 and Cu^+ as well as NO and C_3H_6 coadsorbed on Cu^{2+} in Cu/SiO_2 catalyst.

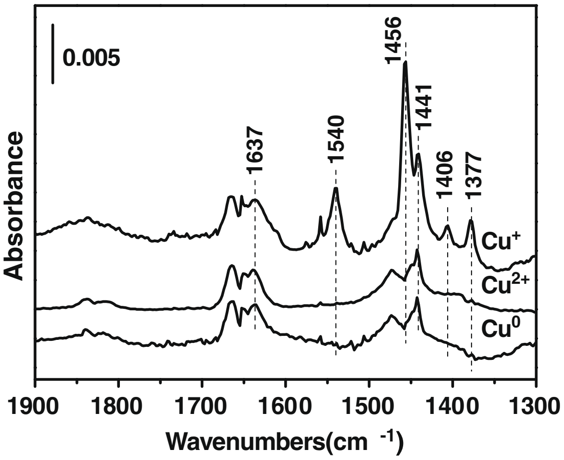

Fig. 10. IR spectra of adsorbed C_3H_6 on Cu^+, Cu^{2+}, and Cu^0 in Cu/SiO_2 catalyst after an evacuation for 1 min. The residual pressure of C_3H_6 is about 70 Pa.

[31]. The red shift of the $\nu_{C=C}$ is about 100 cm^{-1} relative to free $\nu_{C=C}$ in gas phase C_3H_6 (1640 cm^{-1}), suggesting that the C=C bond is evidently activated by Cu^+. It is very possible that this is the effect of π-back donation of d electrons of Cu^+ ions to π* antibonding orbitals of C_3H_6 [31,44].

The IR spectra shown in Fig. 10 are recorded upon the adsorption of C_3H_6 on Cu^+, Cu^{2+}, and Cu^0 in Cu/SiO_2 after an evacuation for one minute (the residual pressure of C_3H_6 is about 70 Pa). When C_3H_6 is adsorbed on Cu^+, the IR bands at 1540, 1456, 1441, 1406, and 1377 cm^{-1} ascribed to C=C interaction with Cu^+, =CH_2 scissoring, =CH_2 scissoring, =C–H in plane bending, and methyl symmetrical C–H bending, respectively, [31,38] are still clearly observed after the evacuation, especially the former two bands. It demonstrates that C_3H_6 is strongly adsorbed on Cu^+ sites. The strength of the adsorbed C_3H_6 on Cu^+ is stronger than CO since it can replace most CO from relatively stable Cu^+CO complex (Fig. 8). However, when C_3H_6 is adsorbed on Cu^0, the result is very different. The characteristic band of adsorbed C_3H_6 (1540 cm^{-1}) is not observed. Only weak bands attributed to gas phase and physisorption of C_3H_6 remain after the evacuation. It seems that C_3H_6 is hardly adsorbed on Cu^0, but from the IR results of the coadsorption between CO and C_3H_6 on Cu^0 (Fig. 8), we can see adsorbed C_3H_6 on Cu^0 is so strong that it can replace most CO from Cu^0CO forms, and the charge transfer between C_3H_6 and Cu^0 also exists since ν_{C-O} is red shifted by about 20 cm^{-1} in the presence of C_3H_6. We consider that C_3H_6 is probably adsorbed parallely on Cu^0 via its C=C bond, according to the selection rules in an IR experiment, this adsorption mode of C_3H_6 may not be detected by IR spectroscopy. The IR spectrum of C_3H_6 adsorbed on Cu^{2+} is almost the same as that of gas phase C_3H_6 and the IR bands almost disappear after the evacuation. Both the IR results of C_3H_6 adsorption alone and NO and C_3H_6 coadsorption suggest that C_3H_6 is hardly adsorbed on Cu^{2+}, namely, the C=C bond of C_3H_6 cannot be activated by Cu^{2+}.

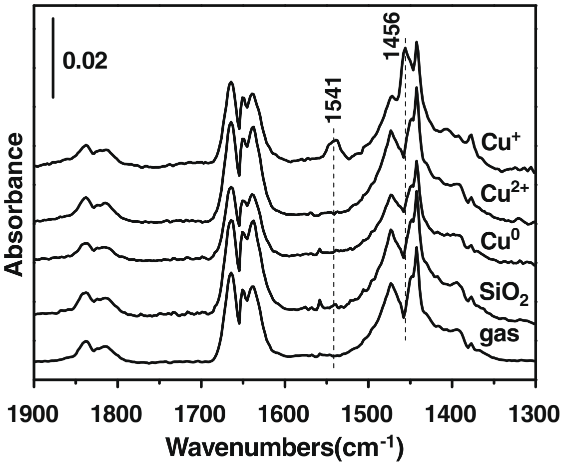

Fig. 9. IR spectra of adsorbed C_3H_6 on Cu^+, Cu^{2+}, and Cu^0 in Cu/SiO_2 catalyst, respectively. For comparison, IR spectra of physisorbed and gas phase C_3H_6 are also presented. The pressure of C_3H_6 is about 270 Pa.

From the reaction results for the oxidation of C_3H_6 by O_2, we find that both Cu^0 and Cu^+ species in Cu/SiO_2 catalyst show C_3H_6 epoxidation activity, and it seems that Cu^0 species is more favorable for PO formation. Cu^{2+} species in Cu/SiO_2 hardly produces PO, but mainly produces acrolein. As we know, the activation of the C=C bond of C_3H_6 is one of the most important steps to generate PO. The result of IR spectrum shown in Fig. 10 indicates that the interaction of C_3H_6 with Cu^+ can greatly weaken the C=C bond: the IR band shifts from 1637 cm^{-1} (position typical of free C_3H_6 molecules) to about 1540 cm^{-1} ($\Delta\nu \approx 100$ cm^{-1}). In Fig. 10 we have not observed the adsorbed C_3H_6 species on Cu^0, however, the interaction between C_3H_6 and Cu^0 still exists because most adsorbed CO molecules on Cu^0 are replaced by C_3H_6 (Fig. 8). The IR results from the coadsorption of CO and C_3H_6 show that π donation of C_3H_6 to Cu^+ or Cu^0 can result in a red shift of ν_{CO} with respect to CO adsorbed on Cu^+ or Cu^0 "solo", too [43]. In addition, π donation of C_3H_6 to Cu^0 is stronger than that to Cu^+ (20 vs. 10 cm^{-1}). Namely, the activation of the C=C bond on Cu^0 is stronger than that on Cu^+. While in the case of Cu^{2+}, C_3H_6 is hardly adsorbed and the C=C bond cannot be activated. Thus, these IR results are in good agreement with those of the fixed bed catalytic reactor experiments. In a word, the more the activation of the C=C bond of C_3H_6, the more the favorableness for PO formation.

We also performed the IR experiments for the coadsorption of CO or NO and C_3H_6 on promoters-modified Cu/SiO_2 catalysts with different valence states of Cu species (spectra not shown). These results are very similar to those of Cu/SiO_2 without modification, and only the intensity of the adsorbed C_3H_6 bands is slightly different. This may be due to the various concentrations of Cu species after modification by promoters. It indicates that the adsorption behavior of C_3H_6 on Cu^0, Cu^+, and Cu^{2+} in Cu/SiO_2 is nearly independent of the promoters (such as KAc, NaAc, KCl, and NaCl). These promoters have little effect on the adsorption and activation of the C=C bond of C_3H_6 on Cu/SiO_2 catalysts, irrespective of the valence states of Cu species. Thus, the role of the promoters in the catalytic performances of the Cu/SiO_2 catalysts has not been explained by the IR experiments.

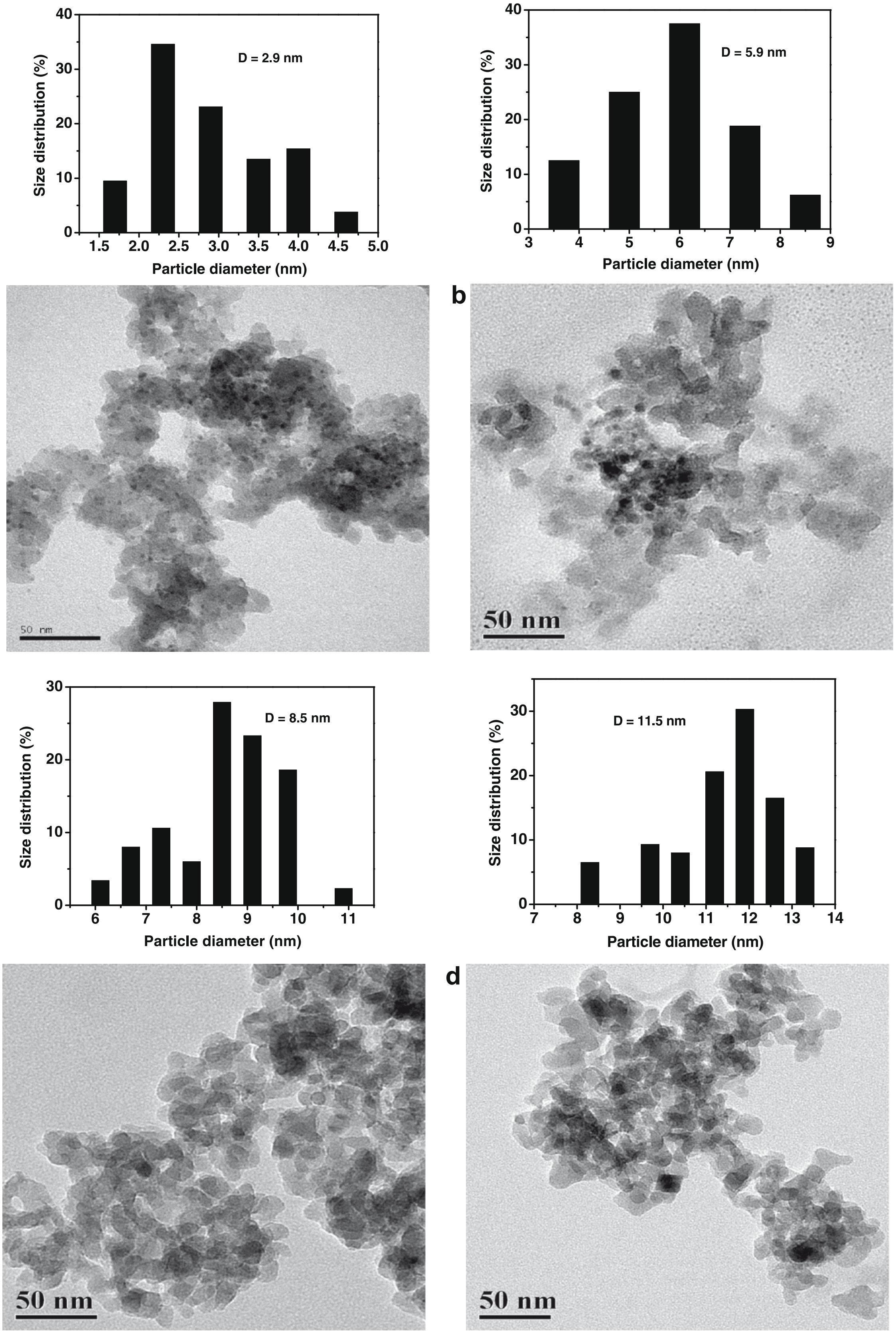

Fig. 11. TEM images of Cu/SiO$_2$ samples calcined at different temperatures with respective particle size distributions. (a) 723 K (2.9 nm), (b) 848 K (5.9 nm), (c) 983 K (8.5 nm), and (d) 1073 K (11.5 nm).

From the above discussion, the catalytic performances on Cu/SiO$_2$ and promoters-modified Cu/SiO$_2$ catalysts are very different, especially for (KAc)–Cu/SiO$_2$ and (NaAc)–Cu/SiO$_2$ catalysts during the low reaction temperatures of the oxidation reaction. However, the IR results show that the activation of the C=C bond of C_3H_6 is independent of the promoters investigated in this work irrespective of Cu^0 or Cu^+ species. We know that the other important factor to create PO is the moderate electrophilic oxygen species. Therefore, besides neutralizing the surface Lewis acidity, we consider that there may exist an interaction between K^+ or Na^+ and Cu species (Cu^0 or Cu^+) [26,28]. The interaction can suppress the reactivity of lattice oxygen species, which are generally regarded to cause the formation of acrolein (the allylic oxidation). Furthermore, the modification by K^+ or Na^+ may stabilize the moderate electrophilic oxygen species generated via the activation of oxygen on the nearby copper sites (Cu^0 or Cu^+) [28]. All these factors are beneficial to PO formation. With raising the reaction temperatures, the Cu^0 or Cu^+ species is probably gradually oxidized to Cu^{2+} species (Supplementary material, Fig. S5), which leads to produce abundant acrolein and CO_x, and the selectivity to PO is largely decreased. However, when KCl or NaCl was used as a modifier, the situation is totally varied. The role of K^+ or Na^+ is already presented above, while the effect of Cl^- on Cu species is much severer. From Figs. 1–3, it is clear that Cl^- ions can result in the agglomeration of Cu species to form agglomerate CuO. In this instance, the concentration of Cu^0 or Cu^+ is greatly diminished. Hence, the conversion of C_3H_6 is rather lower, and the selectivity to PO is also decreased by some extent compared to the catalyst modified by KAc or NaAc, suggesting that larger CuO particle size (15 nm) is not suitable to get PO. Previous investigation shows that NaCl is a good modifier in Ag-based catalysts for C_3H_6 epoxidation reaction to obtain PO [13,16]. They think that NaCl can make the adsorbed oxygen species on the nearby silver sites relatively mildly electrophilic, which is favorable for the epoxidation. However, in our present studies on the Cu/SiO_2 catalysts, the promotive effect of NaCl on producing PO is not so remarkable, at least the promotive effect of NaCl is much inferior to that of KAc.

3.4. Size effect of CuO nanoparticles on the catalytic performances of C_3H_6 epoxidation

Quantum size effect is a very common and important topic in many fields including catalysis. However, the size effect of CuO nanoparticles on the catalytic performances of C_3H_6 epoxidation over Cu-based catalysts has hardly been investigated previously. Fig. 11 indicates the TEM images of Cu/SiO_2 samples calcined at different temperatures with respective particle size distributions. The sizes of CuO particles are adjusted by raising the calcination temperatures from 723 to 1073 K. The CuO particle size in each catalyst is presented in Fig. 11 and is increased from 2.9 to 11.5 nm with the elevated calcination temperatures. According to Scherrer formula $D = K\lambda/(\beta \cos \theta)$, the size of CuO particles in Cu/SiO_2 calcined at 983 K and 1073 K is about 9.1 nm and 15.1 nm, respectively (Supplementary material, Fig. S6). These results are in good agreement with those of TEM images. Tables 2 and 3 show the catalytic performances of Cu/SiO_2 and (KAc)–Cu/SiO_2 catalysts with different CuO particle size for the oxidation of C_3H_6 by O_2, respectively. According to the above results, the Cu/SiO_2 catalyst modified by KAc and pretreated in H_2 shows the highest PO selectivity. Thus, in this series of experiments, we chose KAc as the modifier, and all the Cu/SiO_2 catalysts were pretreated by H_2 before reaction. In Table 2, the rate of PO formation reaches a maximum on the Cu/SiO_2 catalyst with about 5.9 nm CuO particle size (0.44 $mmol\ g^{-1}\ h^{-1}$), and then gradually decreases when the CuO particle size is ranged from about 2.9 to 8.5 nm. Moreover, the combustion product of CO_x is not observed, and the only side product is acrolein. The variety of the acrolein formation rate is just opposite to that of PO. Once the size of CuO particles reaches 11.5 nm, PO is hardly produced at the same reaction temperature. Although the PO formation rate remains 0.14 $mmol\ g^{-1}\ h^{-1}$ due to the higher C_3H_6 conversion at higher reaction temperature, PO selectivity is not more than 10% and CO_x selectivity exceeds 80% (data not shown). The rate of acrolein formation also decreases and the higher C_3H_6 conversion results from the combustion reaction. These results suggest that the size of CuO particles is an absolutely important factor in determining the catalytic performances for C_3H_6 epoxidation reaction. The Cu/SiO_2 catalyst with the size of CuO particles at about 5.9 nm is the most beneficial to generate PO. Once the CuO particle size exceeds 10 nm, the selectivity to PO on this catalyst drops nearly to zero.

Table 2
Catalytic performances of Cu/SiO_2 catalysts with different CuO particle size for the oxidation of C_3H_6 by O_2.

CuO particle size (nm)	*T* (K)	PO formation rate ($mmol\ g^{-1}\ h^{-1}$)	Acrolein formation rate ($mmol\ g^{-1}\ h^{-1}$)
2.9	498	0.26	0.55
5.9	473	0.44	0.16
8.5	498	0.15	0.19
11.5	523	0.14	0.13

Reaction conditions: catalyst volume, 0.2 ml; C_3H_6:O_2:N_2 = 1:1:15; Space velocity = 30,000 h^{-1}. Before reaction, all the catalysts were pretreated by H_2 at 673 K. We chose the reaction temperature at which the PO formation rate reaches the maximum for each catalyst.

Table 3
Catalytic performances of (KAc)–Cu/SiO_2 catalysts with different CuO particle size for the oxidation of C_3H_6 by O_2.

CuO particle size (nm)	*T* (K)	PO formation rate ($mmol\ g^{-1}\ h^{-1}$)	Acrolein formation rate ($mmol\ g^{-1}\ h^{-1}$)
2.9	523	2.50	1.13
5.9	523	0.43	0.20
8.5	523	0.24	0
11.5	573	0.25	0

Reaction conditions: catalyst volume, 0.2 ml; C_3H_6:O_2:N_2 = 1:1:15; Space velocity = 30,000 h^{-1}. Before reaction, all the catalysts were pretreated by H_2 at 673 K. We chose the reaction temperature at which the PO formation rate reaches the maximum for each catalyst.

We also studied the size effect of CuO particles on C_3H_6 epoxidation reaction over (KAc)–Cu/SiO_2 catalysts. In Table 3, the highest rate of PO formation can reach 2.5 $mmol\ g^{-1}\ h^{-1}$ on the (KAc)–Cu/SiO_2 catalyst with the size of CuO particles at about 2.9 nm. This result is the highest in all Cu-based catalysts reported for C_3H_6 epoxidation reaction by O_2 [17,18,25–28]. However, the rates of both PO formation and acrolein formation decrease with the increase of CuO particle size from 2.9 to 11.5 nm. In addition, the decrease of the PO formation rate is very sharp especially when the CuO particle size is increased from about 2.9 to 5.9 nm. Once the size of CuO particles exceeds 8 nm, acrolein is hardly produced. The combustion reaction is predominant and the selectivity to CO_x exceeds 75%. In fact, CO_x is detected on all the (KAc)–Cu/SiO_2 catalysts and the selectivity to CO_x increases fast with the increase of CuO particle size. These phenomena are very different from those observed on the Cu/SiO_2 catalysts. In the case of the (KAc)–Cu/SiO_2 catalyst series which was prepared with the CuO particle size ranging from 2.9 to 11.5 nm, it is found that the smaller the size of the CuO particles, the higher the activity for PO formation. On the other hand, the catalyst with large CuO particle size tends to produce CO_x instead of PO. This may be due to the higher concentration of Cu^+ and Cu^0 species in smaller CuO particles.

Comparing the catalytic performances on Cu/SiO_2 catalysts with and without KAc modification, we find that the rate of PO formation is only slightly enhanced by KAc modification when the CuO particle size is in the ranges of 5.9–11.5 nm. Namely, the effect of KAc modification on PO formation is very small. On the other hand, the rate of acrolein formation is suppressed after the modification by KAc, and CO_x is the main product. These results are quite different from those of the Cu/SiO_2 catalyst with 2.9 nm CuO particle size, on which KAc modification largely increases the rates of PO formation and acrolein formation especially for PO formation. The rate of PO formation is enhanced by about one order after KAc modification. These suggest that the (KAc)–Cu/SiO_2 catalyst with 2.9 nm CuO particle size is a very special sample and is different from other Cu/SiO_2 catalysts. From the above discussion, there is an interaction between Cu species and K^+, which is favorable for PO formation [26]. This interaction may be weaker and weaker with increasing CuO particle size, especially when the size of CuO particles exceeds 6 nm. Thus, in the case of the (KAc)–Cu/SiO_2 catalyst (2.9 nm), the strong interaction between K^+ and Cu species may further stabilize the electrophilic oxygen species [28], which switches the reaction pathway from the formation of acrolein and CO_x to that of PO and leads to high PO selectivity.

4. Conclusions

Both Cu^0 and Cu^+ species in Cu/SiO_2 catalyst show C_3H_6 epoxidation activity. Cu^{2+} species in Cu/SiO_2 hardly produces PO, but mainly produces acrolein and CO_x. IR studies indicate that C_3H_6 is strongly bonded to Cu^0 and Cu^+ sites since most adsorbed CO can be replaced by adsorbed C_3H_6. π donation of C_3H_6 to Cu^+ or Cu^0 results in a red shift of ν_{CO} with respect to CO adsorbed on Cu^+ or Cu^0 “solo”. Moreover, π donation of C_3H_6 to Cu^0 is stronger than that to Cu^+. π-Back donation of d electrons of Cu^+ ions to π^* antibonding orbitals of C_3H_6 also takes place, which results in a distinct C=C bond weakening. C_3H_6 is weakly adsorbed on Cu^{2+}, however, the charge transfer between C_3H_6 and Cu^{2+} is not obvious. KAc is found to be an excellent modifier for PO formation, while Cl^- modification only slightly enhances PO selectivity. The modification by K^+ can switch the main reaction route from allylic oxidation to epoxidation. The small CuO particle size is most favorable for PO formation especially when Cu/SiO_2 sample is modified by KAc, and large CuO particle size tends to produce acrolein and CO_x. The concentration of Cu^0 and Cu^+ species is much higher in small CuO particles. Thus, the isolated Cu species and small CuO_x clusters modified by KAc may be the active sites for C_3H_6 epoxidation reaction using molecular oxygen.

Acknowledgments

This work was financially supported by the National Basic Research Program of China (Grants 2009CB623507), the National Natural Science Foundation of China (NSFC, Grants 20590363), and Program Strategic Scientific Alliances between China and the Netherlands (Grants 2008DFB50130).

Appendix A. Supplementary material

Supplementary data associated with this article can be found, in the online version, at doi:10.1016/j.jcat.2009.09.017.

References

[1] T.A. Nijhuis, M. Makkee, J.A. Moulijn, B.M. Weckhuysen, Ind. Eng. Chem. Res. 45 (2006) 3447.
[2] M.G. Clerici, G. Bellussi, U. Romano, J. Catal. 129 (1991) 159.
[3] Z.W. Xi, N. Zhou, Y. Sun, K.L. Li, Science 292 (2001) 1139.
[4] T. Hayashi, K. Tanaka, M. Haruta, J. Catal. 178 (1998) 566.
[5] A.K. Sinha, S. Seelan, S. Tsubota, M. Haruta, Angew. Chem. Int. Ed. 43 (2004) 1546.
[6] E. Ananieva, A. Reitzmann, Chem. Eng. Sci. 59 (2004) 5509.
[7] Y. Wang, W. Yang, L.J. Yang, X.X. Wang, Q.H. Zhang, Catal. Today 117 (2006) 156.
[8] X.X. Wang, Q.H. Zhang, Q. Guo, Y.C. Lou, L.J. Yang, Y. Wang, Chem. Commun. (2004) 1396.
[9] J.R. Monnier, Appl. Catal. A 221 (2001) 73.
[10] R.P. Wang, X.W. Guo, X.S. Wang, J.Q. Hao, G. Li, J.H. Xiu, Appl. Catal. A 261 (2004) 7.
[11] M.F. Luo, J.Q. Lu, C. Li, Catal. Lett. 86 (2003) 43.
[12] G.J. Jin, G.Z. Lu, Y.L. Guo, Y. Guo, J.S. Wang, X.H. Liu, Catal. Lett. 87 (2003) 249.
[13] G.J. Jin, G.Z. Lu, Y.L. Guo, Y. Guo, J.S. Wang, X.H. Liu, Catal. Today 93 (2004) 173.
[14] R.P. Wang, X.W. Guo, X.S. Wang, J.Q. Hao, Catal. Today 93 (2004) 217.
[15] J.Q. Lu, J.J. Bravo-Suarez, M. Haruta, S.T. Oyama, Appl. Catal. A 302 (2006) 283.
[16] J.Q. Lu, M.F. Luo, H. Lei, C. Li, Appl. Catal. A 237 (2002) 11.
[17] J.Q. Lu, M.F. Luo, H. Lei, X.H. Bao, C. Li, J. Catal. 211 (2002) 552.
[18] J.Q. Lu, M.F. Luo, C. Li, Chin. J. Catal. 25 (2004) 5.
[19] M. Akimoto, K. Ichikawa, E. Echigoya, J. Catal. 76 (1982) 333.
[20] R.L. Cropley, F.J. Williams, O.P.H. Vaughan, A.J. Urquhart, M.S. Tikhov, R.M. Lambert, Surf. Sci. 578 (2005) L85.
[21] R.L. Cropley, F.J. Williams, A.J. Urquhart, O.P.H. Vaughan, M.S. Tikhov, R.M. Lambert, J. Am. Chem. Soc. 127 (2005) 6069.
[22] R.M. Lambert, F.J. Williams, R.L. Cropley, A. Palermo, J. Mol. Catal. A 228 (2005) 27.
[23] D. Torres, N. Lopez, F. Illas, R.M. Lambert, Angew. Chem. Int. Ed. 46 (2007) 2055.
[24] J.R. Monnier, G.W. Hartley, J. Catal. 203 (2001) 253.
[25] O.P.H. Vaughan, G. Kyriakou, N. Macleod, M. Tikhov, R.M. Lambert, J. Catal. 236 (2005) 401.
[26] H. Chu, L. Yang, Q.H. Zhang, Y. Wang, J. Catal. 241 (2006) 225.
[27] W.M. Zhu, Q.H. Zhang, Y. Wang, J. Phys. Chem. C 112 (2008) 7731.
[28] Y. Wang, H. Chu, W.M. Zhu, Q.H. Zhang, Catal. Today 131 (2008) 496.
[29] C.J.G. Vandergrift, P.A. Elberse, A. Mulder, J.W. Geus, Appl. Catal. 59 (1990) 275.
[30] A.R. Balkenende, C.J.G. Vandergrift, E.A. Meulenkamp, J.W. Geus, Appl. Surf. Sci. 68 (1993) 161.
[31] J. Datka, E. Kukulska-Zajac, J. Phys. Chem. B 108 (2004) 17760.
[32] S. Bordiga, R. Buzzoni, F. Geobaldo, C. Lamberti, E. Giamello, A. Zecchina, G. Leofanti, G. Petrini, G. Tozzola, G. Vlaic, J. Catal. 158 (1996) 486.
[33] G. Cordoba, R. Arroyo, J.L.G. Fierro, M. Viniegra, J. Solid State Chem. 123 (1996) 93.
[34] F. Boccuzzi, S. Coluccia, G. Martra, N. Ravasio, J. Catal. 184 (1999) 316.
[35] S. Velu, K. Suzuki, M. Okazaki, M.P. Kapoor, T. Osaki, F. Ohashi, J. Catal. 194 (2000) 373.
[36] M. Haruta, Cattech 6 (2002) 102.
[37] J.M. Coxon, R. Maclagan, A. Rauk, A.J. Thorpe, D. Whalen, J. Am. Chem. Soc. 119 (1997) 4712.
[38] E. Kukulska-Zajac, N. Kumar, T. Salmi, D.Y. Murzin, J. Datka, Catal. Today 100 (2005) 407.
[39] R. Burch, J.P. Breen, F.C. Meunier, Appl. Catal. B 39 (2002) 283.
[40] R. Burch, Phys. Chem. Chem. Phys. 8 (2006) 5483.
[41] K.I. Hadjiivanov, G.N. Vayssilov, Adv. Catal. 47 (2002) 307.
[42] K. Hadjiivanov, H. Knozinger, Phys. Chem. Chem. Phys. 3 (2001) 1132.
[43] J. Datka, E. Kukulska-Zajac, W. Kobyzewa, Catal. Today 114 (2006) 169.
[44] E. Broclawik, P. Rejmak, P. Kozyrac, J. Datka, Catal. Today 114 (2006) 162.